Central Lancashire Online Knowledge (CLoK)

Title	Spectrochemical determination of unique bacterial responses following long-term low-level exposure to antimicrobials
Type	Article
URL	https://clok.uclan.ac.uk/id/eprint/22011/
DOI	https://doi.org/10.1039/c8ay00011e
Date	2018
Citation	Jin, Naifu, Semple, Kirk T., Jiang, Longfei, Luo, Chunling, Martin, Francis L and Zhang, Dayi (2018) Spectrochemical determination of unique bacterial responses following long-term low-level exposure to antimicrobials. Analytical Methods, 10. pp. 1602-1611. ISSN 1759-9660
Creators	Jin, Naifu, Semple, Kirk T., Jiang, Longfei, Luo, Chunling, Martin, Francis L and Zhang, Dayi

It is advisable to refer to the publisher's version if you intend to cite from the work.
https://doi.org/10.1039/c8ay00011e

For information about Research at UCLan please go to http://www.uclan.ac.uk/research/

Spectrochemical determination of unique bacterial responses following long-term low-level exposure to antimicrobials

Naifu Jin[a,b], Kirk T Semple[a], Longfei Jiang[c], Chunling Luo[c], Francis L Martin[d,*], Dayi Zhang[a,b,*]

[a]*Lancaster Environment Centre, Lancaster University, Lancaster LA1 4YQ, UK*

[b]*School of Environment, Tsinghua University, Beijing 100084, China*

[c]*Guangzhou Institute of Geochemistry, Chinese Academy of Sciences, Guangzhou 510640, China*

[d]*School of Pharmacy and Biomedical Sciences, University of Central Lancashire, Preston PR1 2HE, UK*

*Corresponding authors:

Francis L Martin, School of Pharmacy and Biomedical Sciences, University of Central Lancashire, Preston PR1 2HE, UK; Email: flmartin@uclan.ac.uk

Dayi Zhang, School of Environment, Tsinghua University, Beijing 100084, China; Email: zhangdayi@tsinghua.org.cn

18   **ToC graphic**

19

20

21
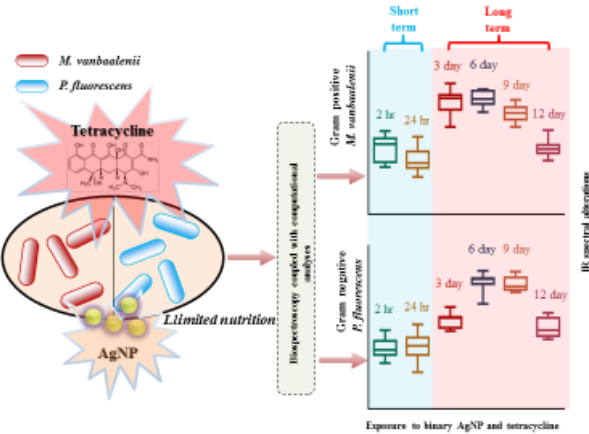
22 **Abstract**

23 Agents arising from engineering or pharmaceutical industries may induce significant

24 environmental impacts. Particularly, antimicrobials not only act as efficient eliminators of

25 certain microbes but also facilitate the propagation of organisms with antimicrobial resistance,

26 raising critical health issues, *e.g.*, the bloom of multidrug-resistant bacteria. Although many

27 investigations have examined microbial responses to antimicrobials and characterized

28 relevant mechanisms, they have focused mainly on high-level and short-term exposures,

29 instead of simulating real-world scenarios in which the antimicrobial exposure is at a low-

30 level for long periods. Herein, we developed a spectrochemical tool, attenuated total

31 reflection Fourier-transform infrared (ATR-FTIR) spectroscopy, as a high-throughput and

32 nondestructive approach to interrogate the long-term effects of low-level antimicrobial

33 exposure in bacterial cells. Post-exposure to nanoparticulate silver (AgNP), tetracycline or

34 their mixtures for 12 days, Gram-positive (*Mycobacterium vanbaalenii* PYR-1) and Gram-

35 negative (*Pseudomonas fluorescens*) bacteria exhibited distinct IR spectral alterations.

36 Multivariate analysis coupled with multivariate regression tree (MRT) indicates nutrient

37 depletion and exposure time as the primary factors in bacterial behaviour, followed by

38 exposure category and bacterial type. Nutrient depletion and starvation during long-term

39 exposure drives bacterial cells into a dormant state or to exhibit additional cellular

40 components (*e.g.*, fatty acids) in response to antimicrobials, consequently causing a broader

41 range of spectral alterations compared to short-term exposure. This work is the first report

42 highlighting the more important roles of exposure duration and nutrient depletion, instead of

43 treatment regimen of antimicrobial, on microbial responses to low-level and prolonged

44 environmental exposures.

45

1. Introduction

Environmental exposure to antimicrobials is a critical issue for both human and microbial communities. Antibiotics are currently ranked as the third most commonly prescribed drugs[1]. In human and veterinary medicine there is abuse of antibiotics, especially for keeping animals healthy at a sub-therapeutic level[2-9]. The primary sink for such antibiotic usage is the environment, *e.g.*, waters and soils, *via* various pathways post-excretion[2, 3 4, 6]. Another group of frequently-used antimicrobial agents is silver-associated entities. Notably, unlike silver ion or salts whose antimicrobial effects are well-studied, the mechanisms of nanoparticulate silver (AgNP) activity remain unclear. However, AgNP is widely exploited for its antibacterial activity, in clothing, food containers, wound dressings, ointments, implant coatings, and ultrafiltration membranes for water purification[10-14]. Developing a reliable approach to interrogate microbial responses to antimicrobials is therefore a matter of urgency, contributing to better understanding of the mechanisms and impacts of antimicrobial agents on environmental microbes[15].

A major issue is the translation from laboratory culture to the real-world scenario of bacteria living in their natural habitats. In contrast to most laboratory culture conditions, *e.g.*, nutrient rich broth, free-living bacteria commonly face nutrient depletion or even more prohibitive circumstances[16]. For instance, cells inhabiting biofilm may be exposed to different concentrations of nutrients, metabolites or environmental stimuli (*e.g.*, temperature, pH, oxygen, etc.)[17-21] across the biofilm matrix and local microenvironment, leading to heterogeneous growth rates and behaviours amongst the cell populations[22, 23]. Amongst these, a small proportion might differentiate into a highly protected phenotypic state and coexist with neighbouring populations that are antibiotic sensitive, resulting from inherent strain differences and adaptation to relatively low concentrations of exposure[16, 22, 23]. Moreover, although regulatory agencies and pharmaceutical administration generally employs high doses of antimicrobials in *in-vivo* and *in-vitro* trials to ensure the safety of test chemicals, residual exposure is typically associated with extremely low-levels in the physical environment; this raises question as to whether high-concentrations of exposure represent the real-world outcomes[24-29]. Thus, research on prolonged low-level exposures of antimicrobials is required in order to shed deeper insights into microbial responses to antimicrobials in the real-world environment[15].

Despite recently developed molecular techniques towards targeting microbial phenotypes, such approaches to identify minor or pre-stage phenotypic alterations induced by low-level exposure remain limited[30-33]. Meanwhile, other confounding factors (*e.g.*, microbial species, growth phase, exposure time, etc.) may also influence test results[16, 31, 34]. In 1991, Fourier-transform infrared (FTIR) spectroscopy was innovatively introduced as a sensitive and rapid screening tool for the characterization, classification and identification of microorganisms[16]. Since then, the emerging application of spectrochemical techniques with computational analysis as an inter-discipline approach shows promising feasibility in microbiology and cytology[30-36]. In the last decade, FTIR spectroscopy plus chemometrics has been exploited broadly for identifying microbial identities, physiologies, activities and related functions[16, 30, 31, 33, 34, 37, 38]. This technical combination provides a major advantage in terms of being high-throughput, label-free and cost-effective in application[30], allowing one to interrogate biological samples *via* a nondestructive and nonintrusive manner, which has great potential in monitoring real-world scenarios[30-32, 34].

The current study applied attenuated total reflection FTIR (ATR-FTIR) microscopy coupled with multivariate analysis to investigate bacterial responses to prolonged low-level exposures of AgNP and tetracycline under nutrient depletion conditions. Compared to short-term exposure, we found that length of exposure plays a more important role than treatment with antimicrobial reagents or bacterial type, further uncovering key influential factors of bacterial responses to antimicrobials during cell growth associated with nutrient depletion.

2. Methodology

2.1 Cell strains and sample preparation

The two bacterial strains used in this study were *Mycobacterium vanbaalenii* PYR-1 (Gram-positive; originally isolated by Carl E Cerniglia and stored in the culture collection https://www.dsmz.de/catalogues/details/culture/DSM-7251.html) and *Pseudomonas fluorescens* (Gram-negative; originally isolated in the laboratory of Kirk T Semple at Lancaster University and gifted for purposes of this study). They were both grown in minimal medium with 20 mM sodium succinate, undertaken in a dark rotary shaker at 150 rpm and the culture temperature was 30±2ºC. After centrifugation and washing with sterile water, cell pellets were diluted in fresh minimal medium with 20 mM sodium succinate and cultivated for about 2 h until they reached the early log-phase (CFU=1×10^7 cells/mL). The four treatments included non-exposure negative control (CK), 4 µg/L of AgNP, 1 µg/L of

5

tetracycline, and a mixture with 4 μg/L of AgNP and 1 μg/L of tetracycline (Binary). The concentrations of AgNP and tetracycline were selected according to their previous reported level in natural environment to mimic the low-level exposure in real-world scenario[38]. They are about 2-4 orders of magnitude lower than the minimum inhibitory concentration (MIC) of AgNP (1 to 10 mg/L)[39, 40] and tetracycline (1 to >30 mg/L)[41, 42], and therefore do not inhibit bacterial growth. The samples of short-term exposure were taken after 2 h (late log-phase, T_0) and 48 h (T_1), respectively. To create a nutrient-depletion condition for long-term exposure, the cells were cultivated in 10-times diluted minimal medium and the culture medium was refreshed every 72 h. The samples were collected at 3 (T_2), 6 (T_3), 9 (T_4) and 12 (T_5) days. The collected cells were then harvested by centrifugation at 4000 rcf for 5 min, washed three times with sterile deionized water, and finally fixed with 70% ethanol to prevent further exposure.

2.2 Spectrochemical analysis

The prepared samples (minimal amount > 5 μL) were then applied onto Low-E slides and dried for analysis by ATR-FTIR spectroscopy. A Bruker TENSOR 27 FTIR spectrometer (Bruker Optics Ltd., UK) with a Helios ATR attachment containing a diamond internal reflection element (IRE) was applied to acquire IR spectra. The data were attained at a resolution of 3.84 cm^{-1}, 2.2 kHz mirror velocity and 32 co-additions. The instrument parameters were set at 32 scans and 16 cm^{-1} resolution. To collect the data, a total of 30 individual spectral measurements were taken randomly from each sample using the aid of the ATR magnification-limited viewfinder camera. Prior to analysing each new specimen, the crystal was cleaned using deionized water and a background reading was taken.

2.3 Multivariate analysis and statistics

All the initial data generated from ATR-FTIR spectroscopy were analysed using MATLAB R2011a (*TheMathsWorks, Natick, MA, USA*) coupled with the IRootLab toolbox (http://irootlab.googlecode.com)[43]. The acquired IR spectra were merged and cut to the biochemical-cell fingerprint region (1800-900 cm^{-1}). Then a rubber-band baseline correction was applied to remove any slopes in this area. The data were then normalized to Amide I (1650 cm^{-1}) and the means were centered allowing alignment of the different spectra for comparison.

Principal component analysis-linear discriminant analysis (PCA-LDA) was applied after data pre-processing to reduce the number of spectra to 10 uncorrelated principal

141 components (PCs), which account for >99% of the total variance. LDA is a suprevised

142 technique coupled with PCA in order to maximize interclass and minimize intraclass

143 varance[30, 31, 44]. Cross-calculation was subsequently performed to mitigate risks resulting from

144 LDA overfitting[45]. The PCA-LDA loadings using (*n*-1) samples (*n* = number of samples in

145 dataset) was trained *via* leave-one-out cross-validation and then calculated the scores of the

146 rest sample. This process was performed for all scores within the test.

147 PCA-LDA cluster vectors are pseudo-spectra highlighting the key biochemical

148 alterations of each group in the dataset[35], which allows one to simplify the identification of

149 discriminating differences amongst groups. The centre of the control cluster itself is moved to

150 the origin of the PCA-LDA factor space. The extent of peak deviation away from the origin

151 of the factor space then occurs according to the centre of each corresponding agent-induced

152 cluster, proportional to the discriminating extent of biochemical differences[31, 45]. Cluster

153 vectors plots were also applied to indicate the most prominent six significant peaks.

154 Multivariate regression trees (MRT) were used to analyse the influence of bacterial

155 type, exposure time and exposure category on biospectral alterations using the R package

156 "mvpart". Herein, Gram-positive (*M. vanbaalenii*) and Gram-negative (*P. fluorescens*) strains

157 were assigned as 1 and 0. The exposure of AgNP, tetracycline and their mixtures were

158 assigned as 1, 2 and 3, respectively. The samples collected at different time points (T_0, T_1, T_2,

159 T_3, T_4 and T_5) were assigned to 1, 2, 3, 4, 5 and 6, respectively.

160 One-way analysis of variance (ANOVA) with Tukey's post-hoc test/or *t*-test was

161 employed to test the differences between treatments. All statistical analyses were carried out

162 in GraphPad Prism 6.

163 **3. Results and discussion**

164 *3.1 Growth-dependent spectrochemical alterations*

165 Throughout the study, a spectral class mean for the bacterial control group has been derived,

166 which generates an average spectrum based on all raw data from the same group. However,

167 minor variability is visualised from the class mean data directly between groups at different

168 time points (Figure 1A and 1B). Although previous studies suggest that bacteria with limited

169 nutrients are more likely to enter a dormant state waiting suitable growth conditions[46, 47], the

170 spectral alterations induced by nutrient depletion are limited. Therefore, a further cluster

171 vectors analysis is applied to highlight the minor alterations derived from nutrient depletion

172 (Figure 1C and 1D). The identical spectral biomarkers in both Gram-positive (*M. Vanbaalenii*)

173 and Gram-negative (*P. fluorescens*) bacteria are associated with Amide I, Amide III (~1204

174 cm^{-1}, ~1647 cm^{-1})[30, 33] (Table 1). The main changes appearing in *M. Vanbaalenii* are Amide

175 III, (~1204 cm^{-1}, ~1400 cm^{-1}), C=N adenine (~1574 cm^{-1}), Amide I (~1652 cm^{-1}), and C=O

176 band (~1725 cm^{-1})[33, 48]. Of these, the amino acid-associated alterations possibly contributing

177 to nucleotide metabolism, which is important for cellular catabolism are significant. Along

178 with long-term starvation and oxygen depletion, decreasing amounts of nucleotides are

179 associated with reduced cell activities and replication compared to log-phase. Furthermore,

180 alterations in other cellular components (*e.g.*, proteins) might be mainly responsible for cell

181 wall maintenance, based on previous study[49].

182   The specific spectrochemical alterations of *P. fluorescens* include Amide III (~1278

183 cm^{-1}), CH_2 bending of the methylene chains in lipids (~1470 cm^{-1}), protein Amide II

184 absorption (~1540 cm^{-1}), C=N cytosine (~1601 cm^{-1}), ν(C=C) lipids, and fatty acids (~1750

185 cm^{-1})[34, 48]. Accordingly, more lipid alterations under nutrient depletion conditions are found

186 in Gram-negative *P. fluorescens versus* Gram-positive *M. vanbaalenii* owing to their

187 differing cell wall structures. There is only a thin peptidoglycan layer (~2-3 nm) between the

188 cytoplasmic and outer membrane in Gram-negative bacteria, whereas the outer membrane in

189 Gram-positive bacteria is a thick peptidoglycan layer of 30 nm with no other additional

190 structure[50]. The attributes of membrane structure may explain the distinct spectrochemical

191 alterations between *P. fluorescens* and *M. vanbaalenii* under nutrient depletion, which might

192 lead to different responses towards long-term exposure of antimicrobials.
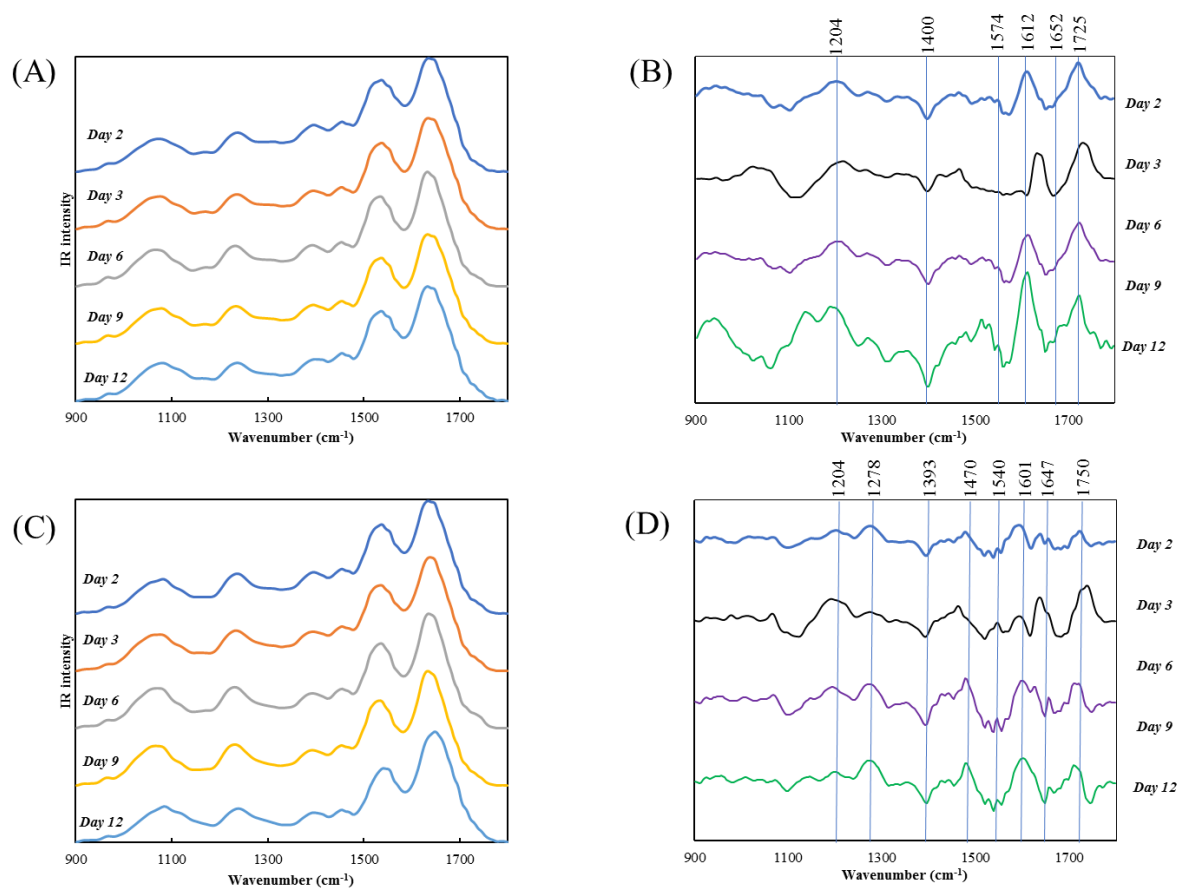
Figure 1. Spectrochemical alterations with length of culture. Infrared spectra of *M. vanbaalenii* (A) and *P. fluorescens* (C) from control group. Cluster vectors plots of *M. vanbaalenii* (B) and *P. fluorescens* (D) from control group, indicating significant wavenumbers contributing to segregating spectral alterations that develop with increasing culture time.

199 **Table 1.** Spectrochemical profile regarding the significant spectral biomarkers peaks derived from cluster vectors of *M. vanbaalenii* (Gram-

200 positive) and *P. fluorescens* (Gram-negative) post-exposure to AgNP, tetracycline and their mixtures. Red dots represent identical biomarkers for

201 both Gram-positive and Gram-negative bacteria, and green and blue dots indicate biomarkers appear only in Gram-positive or Gram-negative

202 bacteria, respectively.

Wavenumber (cm⁻¹)	Annotation	Gram-positive				Gram-negative			
		Growth	AgNP	Tetracycline	Binary	Growth	AgNP	Tetracycline	Binary
~ 964	C-C, C-O deoxyribose	-	●(green)	-	-	-	-	-	-
~ 1084	DNA	-	-	●(green)	●(green)	-	-	-	-
~ 1204	Amide III	●(red)	-	-	-	●(red)	-	-	-
~ 1212	Phosphate	-	●(green)	-	-	-	-	-	-
~ 1220	PO₂⁻ stretching in RNA and DNA	-	-	●(red)	●(red)	-	-	●(red)	-
~ 1278	Amide III	-	-	-	-	●(blue)	-	-	-
~ 1307	Amide III	-	●(green)	-	●(green)	-	-	-	-
~ 1327	Stretching C-N thymine, adenine	-	-	-	-	-	●(blue)	-	●(blue)
~ 1393		-	-	-	-	●(blue)	-	-	-
~ 1400		●(green)	-	-	-	-	-	-	-
~ 1404	CH₃ asymmetric deformation	-	-	-	●(green)	-	-	-	-
~ 1423		-	-	-	-	-	●(blue)	●(blue)	●(blue)
~ 1458	Lipids and proteins	-	-	-	-	-	-	●(blue)	-
~ 1462		-	-	-	●(red)	-	-	-	●(red)
~ 1468		-	-	-	-	-	●(blue)	-	-
~ 1470	CH₂ bending of the methylene chains in lipids	-	-	-	-	●(blue)	-	-	-
~ 1477		-	-	●(green)	-	-	-	-	-
~ 1520	Amide II	-	-	-	-	-	-	-	●(blue)
~ 1540	Protein amide II absorption	-	-	-	-	●(blue)	-	-	-
~ 1555	Ring base	-	●(green)	●(green)	●(green)	-	-	-	-
~ 1574	C=N adenine	●(green)	-	-	-	-	-	-	-
~ 1577	C-C stretch	-	-	-	-	-	●(blue)	-	-

Wavenumber	Assignment								
~ 1601	C=N cytosine	-	-	-	-	● (blue)	-	-	-
~ 1612		● (green)	-	-	-	-	-	-	-
~ 1624		-	-	-	-	-	● (blue)	-	-
~ 1632	C-C stretch	-	-	-	● (green)	-	-	-	-
~ 1639	Amide	-	-	-	-	-	-	● (blue)	-
~ 1647	Amide I	-	-	● (red)	-	● (red)	-	-	-
~ 1652	Amide I	● (green)	-	-	-	-	-	-	-
~ 1666	C=O stretching vibration of pyrimidine base	-	-	-	-	-	● (blue)	-	● (blue)
~ 1670	Amide I	-	● (green)	-	-	-	-	-	-
~ 1694	Proteins	-	-	-	-	-	-	● (blue)	-
~ 1706	C=O thymine	-	● (green)	-	-	-	-	-	-
~ 1725	C=O band	● (green)	-	-	-	-	-	-	-
~ 1740	C=O, lipids	-	-	-	-	-	-	● (blue)	● (blue)
~ 1750	ν(C=C) lipids, fatty acids	-	-	● (red)	-	● (red)	-	-	-

203

204 *3.2 Spectrochemical alterations with long-term AgNP/tetracycline exposure*

205 To identify exposure-induced alterations, the spectral data of each treatment group are

206 compared with the control group at the same time point, eliminating the impacts of cell

207 growth and nutrient depletion (Figure 2*)*. In Gram-positive *M. Vanbaalenii*, the AgNP-

208 induced alterations are C-C, C-O deoxyribose (~964 cm^{-1}), phosphate (~1212 cm^{-1}), Amide

209 III (~1307 cm^{-1}), ring base (~1555 cm^{-1}), Amide I (~1670 cm^{-1}), and C=O thymine (~1706

210 cm^{-1})[30, 33, 38]. Post-exposure to tetracycline, the representative peaks are DNA (~1084 cm^{-1}),

211 PO$_2^-$ stretching in RNA and DNA (~1220 cm^{-1}), ring base (~1555 cm^{-1}), Amide I (~1647

212 cm^{-1}), lipids, and fatty acids (~1750 cm^{-1})[33, 38, 48]. With the binary exposure, the alterations

213 are different from individual exposures, and the specific spectral biomarkers are DNA (~1084

214 cm^{-1}), PO$_2^-$ stretching in RNA and DNA (~1220 cm^{-1}), Amide III (~1307 cm^{-1}), CH$_3$

215 asymmetric deformation (~1404 cm^{-1}, ~1462 cm^{-1}), ring base (~1555 cm^{-1}), and C-C stretch

216 (~1632 cm^{-1})[38, 48]. It is worth mentioning that the binary effects of AgNP and tetracycline on

217 *M. vanbaalenii* spectra are mainly driven by tetracycline as more identical discriminating

218 peaks are observed between these two groups (Table 1). To evaluate the impacts of each

219 exposure, PCA-LDA score plots were generated and illustrate the increasing segregation

220 between groups with increasing exposure time (from day 3 to day 12, Figure 3). Particularly,

221 the biochemical distances of tetracycline and binary groups are co-located, apparently

222 separated from the control group and markedly on day 12. However, the AgNP-treated

223 groups only show slight shifting of biochemical differences compared to the control group.

224 This result is consistent with cluster vectors analysis that the binary-exposure effects in *M.*

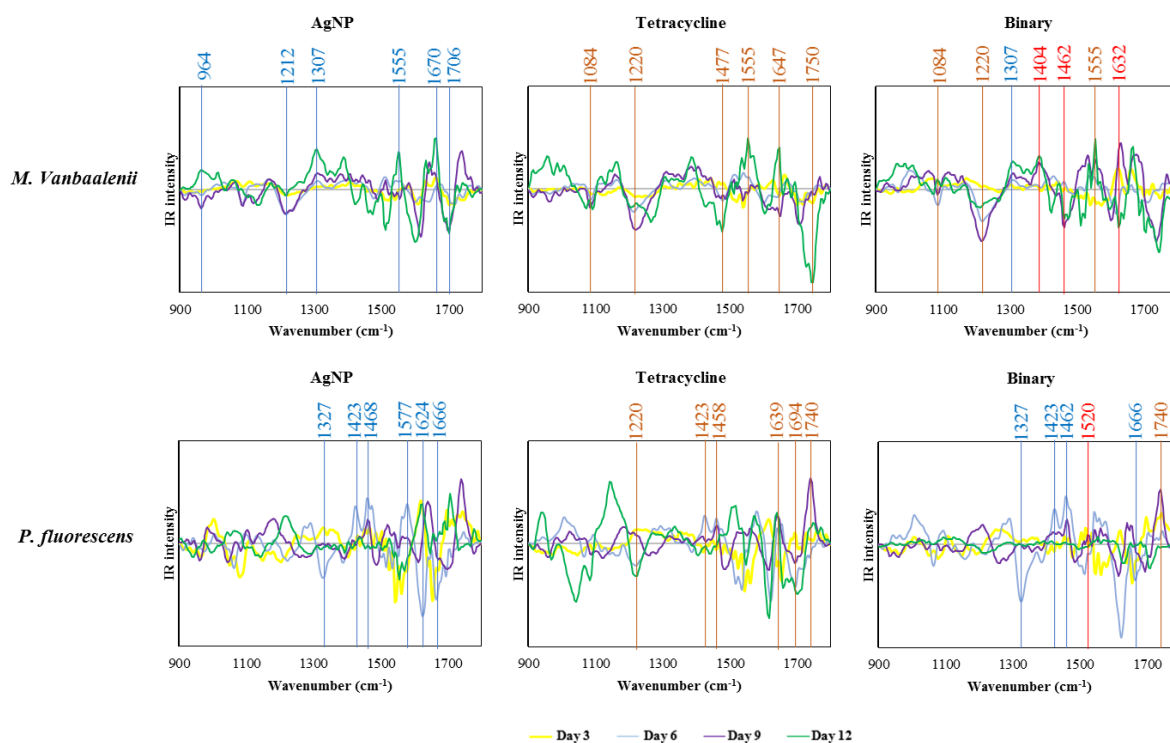225 *vanbaalenii* are closer to tetracycline alone than AgNP.

Figure 2. Cluster vectors plots after PCA-LDA, indicating significant wavenumbers for the segregation of *M. vanbaalenii* and *P. fluorescens* following long-term exposure (day 3 to day 12) to AgNP, tetracycline or their mixtures.
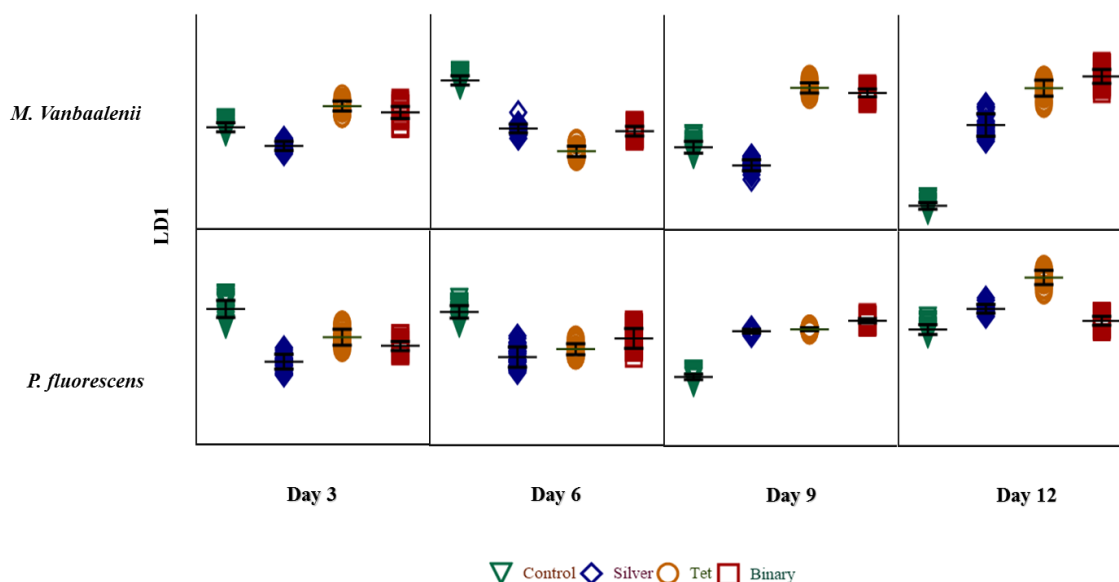

Figure 3. PCA-LDA score plots for the biospectral alteration of *M. vanbaalenii* and *P. fluorescens* following long-term exposure (day 3 to day 12) to AgNP, tetracycline or their mixtures.

235 In Gram-negative *P. fluorescens*, all the exposure groups are clearly separated from the

236 control group in the PCA-LDA score plots (Figure 3), and there is no significant difference

237 between each treatment. The AgNP-induced alterations include stretching C-N thymine,

238 adenine (~1327 cm^{-1}), lipids and proteins (~1458 cm^{-1}), C-C stretch (~1577 cm^{-1}), (~1624

239 cm^{-1}), and C=O stretching vibration of pyrimidine base (~1666 cm^{-1})[48]. The tetracycline-

240 induced peaks are DNA (~1220 cm^{-1}); (~1423 cm^{-1}), collagen (~1458 cm^{-1}), Amide I (~1639

241 cm^{-1}, ~1694 cm^{-1}), and C=O lipids (~1740 cm^{-1})[38, 48]. Generally, outer cellular components

242 are widely affected by both AgNP and tetracycline, including Amides I/II and proteins

243 (~1307 cm^{-1}, ~1647 cm^{-1}, 1639 -1694 cm^{-1}), and lipids and/or fatty acids (1750 cm^{-1}, 1458

244 cm^{-1}, 1740 cm^{-1})[30, 33, 38, 48], indicating that the cell membrane is the primary reactive target

245 associated with both antimicrobials which penetrate bacterial cells *via* passive diffusion and

246 inhibit bacterial growth by perturbing protein synthesis or altering membrane structure[51].

247 Additionally, more inner cellular components are identified to be associated with tetracycline

248 exposure than AgNP, *e.g.*, inherent DNA and RNA, possibly due to the antibiotic mechanism

249 of tetracycline which blocks the elongation cycle by preventing incoming aminoacyl-tRNA

250 (aa-tRNA) from binding to the ribosomal A-site and inhibiting protein synthesis[52]. Different

251 from Gram-positive strains, AgNP-induced alterations contribute predominantly to the binary

252 effects in *P. fluorescens*, *i.e.*, stretching C-N thymine, adenine (~1327 cm^{-1}, ~1423 cm^{-1},

253 ~1462 cm^{-1}), Amide II (~1520 cm^{-1}), C=O stretching vibration of pyrimidine base (~1666

254 cm^{-1}), and C=O lipids (~1740 cm^{-1})[31, 34]. These findings imply the antimicrobial synergism

255 of AgNP and tetracycline. A previous study suggests that antibiotics' efficacy against

256 microbes may increase in the presence of AgNP because of the bonding reaction between

257 antibiotics and nanofillers, owing to the chelating reaction of hydroxyl and amide groups in

258 antibiotic molecules with AgNP[53].

3.3 Impacts of exposure time on spectrochemical alterations

260 Although short-term impacts by antimicrobials on bacteria is obvious and well-studied, their

261 consequences may last for extended periods and remain unknown[54]. To unravel such long-

262 term exposure effects, we measured the biospectral alterations at different time points, and

263 found distinguishing biomarkers post-exposure to antimicrobials between short-term *versus*

264 long-term treatments (Figure 4). Generally, in short-term exposure (≤3 days), spectral

265 changes are associated with components from cell membranes wherein most antimicrobial-

266 induced alterations occur in both strains, including glycogen (~1022 cm^{-1}), symmetric

267 phosphate stretching vibrations ($\nu_s PO_2^-$; ~1088 cm^{-1}, 1092 cm^{-1}), carbohydrates (~1165

268 cm^{-1}), protein phosphorylation (~964 cm^{-1}), Amide I (~1609 cm^{-1}, 1612 cm^{-1}, 1659 cm^{-1},

269 ~1670 cm^{-1}), Amide III (~1269 cm^{-1}), COO- symmetric stretching vibrations of fatty acids

270 and amino acid (~1408 cm^{-1}), proteins (~1485 cm^{-1}, ~1550 cm^{-1}, ~1650 cm^{-1}), and lipids

271 (~1701 cm^{-1}, 1705-1750 cm^{-1})[30, 32, 38, 48]. Besides external cellular components, some

272 inherent elements are significantly influenced in long-term exposure (>3 days). For instance,

273 long-term tetracycline-induced alterations in *P. fluorescens* include RNA and DNA (*e.g.*,

274 ~1220 cm^{-1}, ~1423 cm^{-1}). Compared to prolonged exposure, short exposure induces minimal

275 alterations, possibly owing to bacteria undergoing pre-stage reactions against antimicrobials.

276 During extended exposure periods, the more obvious biospectral alterations might be

277 explained by increasing tetracycline accumulation *via* penetration and stronger antibiotic

278 effects, which prevent RNA binding to the ribosomal A-site and protein synthesis[52], and

279 further inhibit RNA/DNA synthesis and duplication[55]. Another explanation is the post-

280 antibiotic effect (PAE) or lag of bacterial regrowth induced by long-term antimicrobial

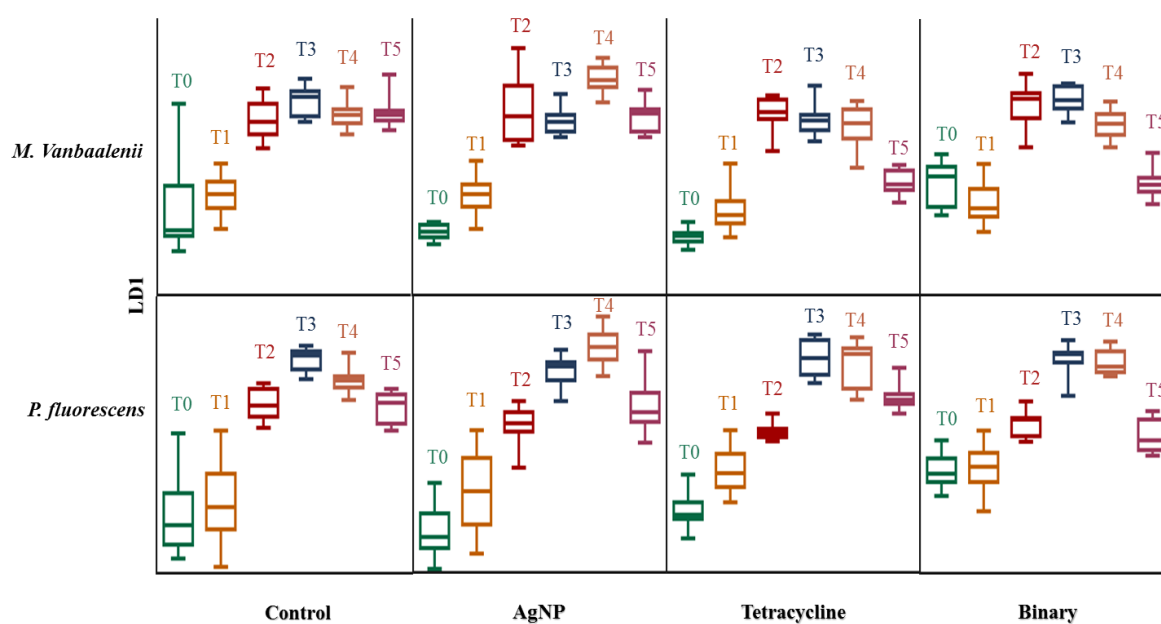281 exposure, driving bacterial entry into a growth suppression state[56, 57].

282

283 **Figure 4.** PCA-LDA score plots of the biospectral alteration of *M. vanbaalenii* and *P.*

284 *fluorescens* in both short-term and long-term exposure to AgNP, tetracycline and their

285 mixtures. T_0, T_1, T_2, T_3, T_4 and T_5 represent exposure time of 2 h, 2 days, 3 days, 6 days, 9

286 days and 12 days, respectively.

287

288   *3.4 Influential factors determining bacterial long-term responses to antimicrobials*

289   Although distinct impacts of different antimicrobials on bacteria have been well-documented,
290   many variables including intrinsic and external factors may alter such influences in real-
291   world scenarios. In the present study, we evaluated bacterial type, exposure category,
292   exposure time and nutrient depletion, but which factor is the most dominating remains
293   unlcear. To answer this question, a multivariate regression trees (MRT) analysis based on
294   isolated discriminating biomarkers is conducted to quantify the impacts of these four factors
295   on spectral alterations. MRT visualizes these influencing factors on spectral variations in a
296   tree with four splits based on exposure time, exposure category, bacterial type and nutrient
297   depletion, explaining 63.7% of the total spectral variance (Figure 5). Level of influence is
298   ranked as exposure time > exposure type > bacterial type = nutrient depletion. Exposure time
299   accounts for 17.8% of the total variance, with the first split separating the group of 12-day
300   exposure owing to the relatively lower intensities of DNA. In the 12-day exposure group,
301   exposure category explains 16.1% of the variance and splits spectra into two groups of
302   control/tetracycline and AgNP/binary, mainly based on DNA spectral biomarkers. The group
303   of exposure <12 days is further split by bacterial type, accounting for 14.9% of the total
304   variance and attributed to differences in DNA, phospholipid-derived fatty acids and proteins.
305   The final split representing nutrient depletion separates the groups of 6-9 day and 0-3 day for
306   Gram-positive bacteria (*M. vanbaalenii*, 14.9%), owing to higher cellular activities reflected
307   by significant variations in DNA, phospholipid-derived fatty acids and proteins.

308   The MRT results are consistent with PCA-LDA score plots (Figure 4). The spectral
309   distances of *P. fluorescens*, for instance, are similar regardless of exposure categories from
310   day 9 due to cell regeneration against the exposure and exhibiting resistance to
311   antimicrobials[46]. A prior study reported that long-term exposure (5 days) to 1 μg/L of
312   tetracycline shows no apparent effect on cyanobacterial cells due to their natural variability in
313   tetracycline resistance[58]. It might explain the closer distance between groups of control and
314   tetracycline. Moreover, the distinct behaviours of *M. vanbaalenii* and *P. fluorescens* upon
315   starvation can explain the fourth split in MRT, *i.e.*, *M. vanbaalenii* enters a replicative state
316   after 6-day exposure to adapt to conditions of insufficient nutrients, whereas *P. fluorescens*
317   appears more susceptible to nutrient depletion and starts regrowth. Evidence can be found
318   from the additional collular components produced in Gram-negative *P. fluorescens*, *e.g.*, fatty
319   acids (~1750 cm^{-1}), as their predominant energy to survive[46].
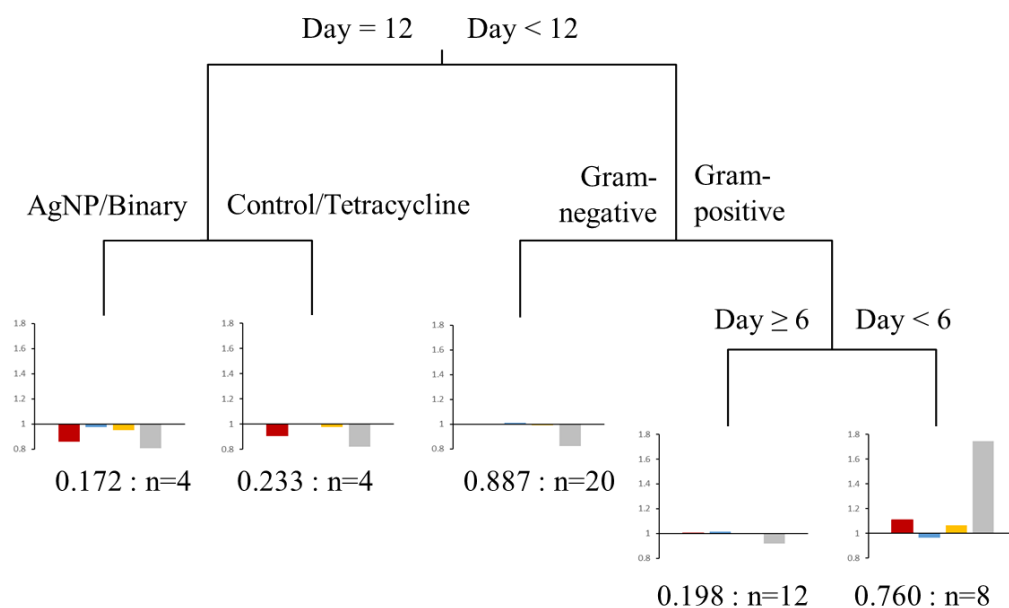
Error: 0.364 CV Error: 0.572 SE: 0.119

Figure 5. Multivariate regression tree (MRT) analysis of environmental variables explaining discriminating biomarkers. The scale of the sub-figures reflects the alteration degree (number one represents the average level). Red bars represent biomarkers assigned to DNA; blue bars represent biomarkers associated with proteins; yellow bars represent biomarkers assigned to phospholipid-derived fatty acids; and, grey bars represent other cellular components.

Moreover, bacterial type may also have impacts on the consequences posed by antimicrobials since bacteria differ in their cellular structures. Antimicrobials acting as both efficient eliminators to microbes and selective agents help to propagate organisms with resistance ability[59]. Herein, we found discriminating alterations between Gram-positive and Gram-negative strains within the same exposure treatment. All the treatments exhibit distinct alterations in Gram-positive *M. vanbaalenii* under nutrient depletion conditions (Day 3 to Day 12), although AgNP generates very limited impact as compared to tetracycline or binary exposure groups; these are not observed in *P. fluorescens*. The results from PCA-LDA scores plots (Figure 3) and MRT (Figure 5) also show induced alterations in *M. vanbaalenii* are significant compared to *P. fluorescens*. Furthermore, after long-term exposure (12 days),

17

337   Gram-negative *P. fluorescens* exhibit a broad range of spectral alterations assigned to lipids

338   and/or fatty acid (*e.g.*, 1458 cm^{-1}, 1740 cm^{-1}), which are absent in Gram-positive *M.*

339   *vanbaalenii*, mainly attributed to their different cell wall structures. The rigidity and extended

340   cross-linking may reduce the target sites in cell membranes for environmental exposures and

341   afford further protection to cells from antimicrobial penetration[12, 53]. It implies that cell

342   membranes of Gram-negative bacteria are more likely to be influenced compared to Gram-

343   positive bacteria under certain antibacterial treatments (*e.g.*, AgNP)[12, 50, 60]. Past studies report

344   the oxidation of smaller AgNPs (1-10 nm) by intercellular reactive oxygen species (ROS) in

345   Gram-negative bacteria, resulting in the release of silver ions during AgNP penetration

346   through the cell membrane and entrance into the cytoplasm[60]. These silver ions could be

347   further transferred to other Gram-negative bacterial cells, the membrane and cytoplasm which

348   contain many sulfur-containing proteins for the released Ag^+ to bind to and inactivate[50, 60].

349   Furthermore, it has been recognised that heavy metal treatment can induce global

350   biomolecular changes in lipids and proteins, implying exotic exposure may lead to the

351   development of relevant metabolic changes in cellular components, particularly the

352   membrane[61-63]. A recent study, for instance, reported that Ag exposure could increase cellular

353   lipid contents while decrease membrane fluidity[61], and the possible mechanism is upregulated

354   lipid biosynthesis, which is known to be associated with the reduced membrane permeability.

355   Besides bacterial type, exposure time and exposure category, nutrient depletion is also

356   found to be an influential factor in the bacterial antimicrobial response. Here, bacterial cells

357   tend to adapt to new environmental stimuli after entering into a long-term nutrient-deprived

358   situation. From the cluster vectors analysis (Figure 1), spectral alterations in both strains from

359   Day 6 show slight peak shifts, which can be regarded as a potential signal showing that

360   bacterial cells are undergoing adaption. Additionally, *M. vanbaalenii* becomes a persistent

361   suspension in the media on entering a dormant state from Day 6. This is because bacteria in a

362   non-growing state can survive for much longer time under conditions of reduced oxygen or

363   nutrient deprivation[46, 47]. Upon starvation, bacterial cells fragment into small spheroids

364   exhibiting rapid and drastic decreases in endogenous metabolism. This reorganization gives

365   bacteria maximum survival during long-term starvation. Specifically, bacteria on starvation

366   initially induce dwarfing generating cell number increases *via* fragmentation over the first 1

367   to 2 h and continuous size reductions in the fragmented cells, but no further increase in

368   numbers. After dwarfing phases, cell size continues to get smaller, with little or no metabolic

369   activity, and slow loss of viability[64]. It has been reported that non-growing phase bacteria

370 adapt to and increase their tolerance to environmental stresses and such developed persistent

371 bacilli are capable of surviving several months of combinatorial antibiotic treatment[47], which

372 implies that stressed living conditions, to some extent and paradoxically, could help microbial

373 resistance to antimicrobial effects.

4. Conclusions

375 In the present study, we employed spectrochemical analysis coupled with multivariate

376 analysis as a robust tool towards investigating bacterial responses[65] to long-term and low-

377 level exposure of antimicrobials under nutrient depletion conditions. ATR-FTIR spectroscopy

378 shows feasibility in revealing sufficient biochemical information continuously even at

379 extremely low-level exposures in a starvation situation, which fits better with real-world

380 circumstances and the natural state of microcosms. From the multivariate analysis of spectra

381 coupled with MRT, we evaluate the significance of different factors on long-term bacterial

382 responses to antimicrobials and find pivotal roles for exposure time and nutrient depletion.

383 Nutrient depletion can drive bacterial cells to either enter into a dormant state or exhibit

384 extra-cellular components against environmental antimicrobials, consequently causing a

385 broader range of spectral alteration compared to short-term exposures. Differences in

386 bacterial behaviours towards antimicrobials are also found between bacterial types (Gram-

387 positive *versus* Gram-negative) attributed to variations in cell wall structure. Our work is the

388 first revealing of the more important roles of exposure duration and nutrient depletion, rather

389 than of antimicrobial reagents, on microbial responses to low-level and prolonged

390 environmental exposures. We believe this approach has an important future with potential

391 feasibility in *in situ* screening of environmental exposures in real-time.

Conflicts of interest

393 There are no conflicts of interest to declare.

Acknowledgement

396

397

398

References

1. J. Conly, *Can. Med. Assoc. J.*, 2002, **167**, 885-891.
2. J. W. Harrison and T. A. Svec, *Quintessence Int.*, 1998, **29**, 223-229.
3. J. C. Chee-Sanford, R. I. Aminov, I. J. Krapac, N. Garrigues-Jeanjean and R. I. Mackie, *Appl. Environ. Microbiol.*, 2001, **67**, 1494-1502.
4. G. Hamscher, S. Sczesny, H. Hoper and H. Nau, *Anal Chem*, 2002, **74**, 1509-1518.
5. X. L. Ji, Q. H. Shen, F. Liu, J. Ma, G. Xu, Y. L. Wang and M. H. Wu, *J. Hazard Mater.*, 2012, **235**, 178-185.
6. L. Cantas, S. Q. A. Shah, L. M. Cavaco, C. M. Manaia, F. Walsh, M. Popowska, H. Garelick, H. Burgmann and H. Sorum, *Front. Microbiol.*, 2013, **4**, 14.
7. A. Koluman and A. Dikici, *Crit. Rev. Microbiol.*, 2013, **39**, 57-69.
8. M. Tandukar, S. Oh, U. Tezel, K. T. Konstantinidis and S. G. Pavlostathis, *Environ. Sci. Technol.*, 2013, **47**, 9730-9738.
9. J. L. Martinez and F. Baquero, *Ups. J. Med. Sci.*, 2014, **119**, 68-77.
10. J. S. Kim, E. Kuk, K. N. Yu, J. H. Kim, S. J. Park, H. J. Lee, S. H. Kim, Y. K. Park, Y. H. Park, C. Y. Hwang, Y. K. Kim, Y. S. Lee, D. H. Jeong and M. H. Cho, *Nanomed.-Nanotechnol. Biol. Med.*, 2014, **10**, 1119-1119.
11. C. N. Lok, C. M. Ho, R. Chen, Q. Y. He, W. Y. Yu, H. Sun, P. K. H. Tam, J. F. Chiu and C. M. Che, *J. Biol. Inorg. Chem.*, 2007, **12**, 527-534.
12. H. H. Lara, N. V. Ayala-Nunez, L. D. I. Turrent and C. R. Padilla, *World J. Microbiol. Biotechnol.*, 2010, **26**, 615-621.
13. C. Marambio-Jones and E. M. V. Hoek, *J. Nanopart. Res*, 2010, **12**, 1531-1551.
14. R. J. Griffitt, N. J. Brown-Peterson, D. A. Savin, C. S. Manning, I. Boube, R. A. Ryan and M. Brouwer, *Environ. Toxicol. Chem.*, 2012, **31**, 160-167.
15. A. Gupta and S. Silver, *Nat. Biotechnol.*, 1998, **16**, 888-888.
16. N. F. Jin, D. Y. Zhang and F. L. Martin, *Integr. Biol.*, 2017, **9**, 406-417.
17. P. Marschner, C. H. Yang, R. Lieberei and D. E. Crowley, *Soil Biol Biochem*, 2001, **33**, 1437-1445.
18. E. K. Costello, C. L. Lauber, M. Hamady, N. Fierer, J. I. Gordon and R. Knight, *Science*, 2009, **326**, 1694-1697.
19. C. L. Lauber, M. Hamady, R. Knight and N. Fierer, *Appl. Environ. Microbiol.*, 2009, **75**, 5111-5120.
20. M. Wietz, B. Wemheuer, H. Simon, H. A. Giebel, M. A. Seibt, R. Daniel, T. Brinkhoff and M. Simon, *Environ. Microbiol.*, 2015, **17**, 3822-3831.
21. H. Li, F. L. Martin and D. Y. Zhang, *Anal. Chem.*, 2017, **89**, 3909-3918.
22. P. S. Stewart and J. W. Costerton, *Lancet*, 2001, **358**, 135-138.
23. N. Hoiby, T. Bjarnsholt, M. Givskov, S. Molin and O. Ciofu, *Int. J. Antimicrob. Agents*, 2010, **35**, 322-332.
24. C. G. Mayhall and E. Apollo, *Antimicrob. Agents Chemother.*, 1980, **18**, 784-788.
25. M. R. W. Brown, D. G. Allison and P. Gilbert, *J. Antimicrob. Chemother.*, 1988, **22**, 777-780.
26. S. M. Ede, L. M. Hafner and P. M. Fredericks, *Appl. Spectrosc.*, 2004, **58**, 317-322.
27. O. I. Kalantzi, R. Hewitt, K. J. Ford, L. Cooper, R. E. Alcock, G. O. Thomas, J. A. Morris, T. J. McMillan, K. C. Jones and F. L. Martin, *Carcinogenesis*, 2004, **25**, 613-622.
28. J. L. Barber, M. J. Walsh, R. Hewitt, K. C. Jones and F. L. Martin, *Mutagenesis*, 2006, **21**, 351-360.
29. O. Fridman, A. Goldberg, I. Ronin, N. Shoresh and N. Q. Balaban, *Nature*, 2014, **513**, 418-421.

448 30. F. L. Martin, J. G. Kelly, V. Llabjani, P. L. Martin-Hirsch, Patel, II, J. Trevisan, N. J.
449 Fullwood and M. J. Walsh, *Nat. Protoc.*, 2010, **5**, 1748-1760.
450 31. M. J. Riding, F. L. Martin, J. Trevisan, V. Llabjani, Patel, II, K. C. Jones and K. T.
451 Semple, *Environ. Pollut.*, 2012, **163**, 226-234.
452 32. J. Li, R. Strong, J. Trevisan, S. W. Fogarty, N. J. Fullwood, K. C. Jones and F. L.
453 Martin, *Environ. Sci. Technol.*, 2013, **47**, 10005-10011.
454 33. M. J. Baker, J. Trevisan, P. Bassan, R. Bhargava, H. J. Butler, K. M. Dorling, P. R.
455 Fielden, S. W. Fogarty, N. J. Fullwood, K. A. Heys, C. Hughes, P. Lasch, P. L.
456 Martin-Hirsch, B. Obinaju, G. D. Sockalingum, J. Sule-Suso, R. J. Strong, M. J.
457 Walsh, B. R. Wood, P. Gardner and F. L. Martin, *Nat. Protoc.*, 2014, **9**, 1771-1791.
458 34. K. A. Heys, M. J. Riding, R. J. Strong, R. F. Shore, M. G. Pereira, K. C. Jones, K. T.
459 Semple and F. L. Martin, *Analyst*, 2014, **139**, 896-905.
460 35. J. G. Kelly, J. Trevisan, A. D. Scott, P. L. Carmichael, H. M. Pollock, P. L. Martin-
461 Hirsch and F. L. Martin, *J. Proteome Res.*, 2011, **10**, 1437-1448.
462 36. J. Trevisan, P. P. Angelov, P. L. Carmichael, A. D. Scott and F. L. Martin, *Analyst*,
463 2012, **137**, 3202-3215.
464 37. N. Jin, M. Paraskevaidi, K. T. Semple, F. L. Martin and D. Y. Zhang, *Anal Chem*,
465 2017, **89**, 9814-9821.
466 38. N. Jin, K. T. Semple, L. Jiang, C. Luo, D. Zhang and F. L. Martin, *Analyst*, 2018, **143**,
467 768-776.
468 39. S. N. El Din, T. A. El-Tayeb, K. Abou-Aisha and M. El-Azizi, *Int. J. Nanomed.*, 2016,
469 **11**, 1749-1758.
470 40. A. J. Kora and J. Arunachalam, *World J. Microbiol. Biotechnol.*, 2011, **27**, 1209-1216.
471 41. J. T. H. Jo, F. S. L. Brinkman and R. E. W. Hancock, *Antimicrob. Agents Chemother.*,
472 2003, **47**, 1101-1111.
473 42. H. Wu, X. Shi, H. Wang and J. Liu, *J. Antimicrob. Chemother.*, 2000, **46**, 121-123.
474 43. J. Trevisan, P. P. Angelov, A. D. Scott, P. L. Carmichael and F. L. Martin,
475 *Bioinformatics*, 2013, **29**, 1095-1097.
476 44. F. L. Martin, M. J. German, E. Wit, T. Fearn, N. Ragavan and H. M. Pollock, *J.*
477 *Comput. Biol.*, 2007, **14**, 1176-1184.
478 45. J. Li, G. G. Ying, K. C. Jones and F. L. Martin, *Analyst*, 2015, **140**, 2687-2695.
479 46. J. C. Betts, P. T. Lukey, L. C. Robb, R. A. McAdam and K. Duncan, *Mol. Microbiol.*,
480 2002, **43**, 717-731.
481 47. T. Hampshire, S. Soneji, J. Bacon, B. W. James, J. Hinds, K. Laing, R. A. Stabler, P.
482 D. Marsh and P. D. Butcher, *Tuberculosis*, 2004, **84**, 228-238.
483 48. Z. Movasaghi, S. Rehman and I. U. Rehman, *Appl. Spectrosc. Rev.*, 2008, **43**, 134-
484 179.
485 49. M. Drapal, P. R. Wheeler and P. D. Fraser, *Microbiology-(UK)*, 2016, **162**, 1456-1467.
486 50. J. R. Morones, J. L. Elechiguerra, A. Camacho, K. Holt, J. B. Kouri, J. T. Ramirez
487 and M. J. Yacaman, *Nanotechnology*, 2005, **16**, 2346-2353.
488 51. D. Schnappinger and W. Hillen, *Arch. Microbiol.*, 1996, **165**, 359-369.
489 52. S. R. Connell, C. A. Trieber, G. P. Dinos, E. Einfeldt, D. E. Taylor and K. H.
490 Nierhaus, *Embo J.*, 2003, **22**, 945-953.
491 53. A. M. Fayaz, K. Balaji, M. Girilal, R. Yadav, P. T. Kalaichelvan and R. Venketesan,
492 *Nanomed.-Nanotechnol. Biol. Med.*, 2010, **6**, 103-109.
493 54. C. Jernberg, S. Lofmark, C. Edlund and J. K. Jansson, *Microbiology-(UK)*, 2010, **156**,
494 3216-3223.
495 55. M. Argast and C. F. Beck, *Antimicrob. Agents Chemother.*, 1984, **26**, 263-265.
496 56. R. W. Bundtzen, A. U. Gerber, D. L. Cohn and W. A. Craig, *Rev. Infect. Dis.*, 1981, **3**,
497 28-37.

498   57.   K. Fuursted, A. Hjort and L. Knudsen, *J. Antimicrob. Chemother.*, 1997, **40**, 221-226.
499   58.   F. Pomati, A. G. Netting, D. Calamari and B. A. Neilan, *Aquat. Toxicol.*, 2004, **67**,
500   387-396.
501   59.   S. B. Levy, *J. Antimicrob. Chemother.*, 2002, **49**, 25-30.
502   60.   Z. M. Xiu, J. Ma and P. J. J. Alvarez, *Environ Sci Technol*, 2011, **45**, 9003-9008.
503   61.   R. Gurbanov, S. N. Ozek, S. Tunçer, F. Severcan and A. G. Gozen, *J. Biophotonics*,
504   2017, Doi: 10.1002/jbio.201700252.
505   62.   R. Gurbanov, N. Simsek Ozek, A. G. Gozen and F. Severcan, *Anal Chem*, 2015, **87**,
506   9653-9661.
507   63.   M. Kardas, A. G. Gozen and F. Severcan, *Aquat Toxicol*, 2014, **155**, 15-23.
508   64.   S. Kjelleberg, B. A. Humphrey and K. C. Marshall, *Appl. Environ. Microbiol.*, 1983,
509   **46**, 978-984.

510   65.   M. J. Riding, J. Trevisan, C. J. Hirschmugl, K. C. Jones, K. T. Semple and F. L.
511   Martin, *Environ. Int.*, 2012, **50,** 56-65.

512

513